

Research Article

Numerical and Experimental Investigation of Air Cooling for Photovoltaic Panels Using Aluminum Heat Sinks

Zainal Arifin , **Dominicus Danardono Dwi Prija Tjahjana**, **Syamsul Hadi**,
Rendy Adhi Rachmanto, **Gabriel Setyohandoko**, and **Bayu Sutanto**

Department of Mechanical Engineering, Universitas Sebelas Maret, Surakarta 57126, Indonesia

Correspondence should be addressed to Zainal Arifin; zainal_arifin@staff.uns.ac.id

Received 14 October 2019; Revised 10 December 2019; Accepted 18 December 2019; Published 10 January 2020

Academic Editor: Alberto Álvarez-Gallegos

Copyright © 2020 Zainal Arifin et al. This is an open access article distributed under the Creative Commons Attribution License, which permits unrestricted use, distribution, and reproduction in any medium, provided the original work is properly cited.

An increase in the operating temperature of photovoltaic (PV) panels caused by high levels of solar irradiation can affect the efficiency and lifespan of PV panels. This study uses numerical and experimental analyses to investigate the reduction in the operating temperature of PV panels with an air-cooled heat sink. The proposed heat sink was designed as an aluminum plate with perforated fins that is attached to the back of the PV panel. A comprehensive computational fluid dynamics (CFD) simulation was conducted using the software ANSYS Fluent to ensure that the heat sink model worked properly. The influence of heat sinks on the heat transfer between a PV panel and the circulating ambient air was investigated. The results showed a substantial decrease in the operating temperature of the PV panel and an increase in its electrical performance. The CFD analysis in the heat sink model with an air flow velocity of 1.5 m/s and temperature of 35°C under a heat flux of 1000 W/m² showed a decrease in the PV panel's average temperature from 85.3°C to 72.8°C. As a consequence of decreasing its temperature, the heat sink increased the open-circuit photovoltage (V_{OC}) and maximum power point (P_{MPP}) of the PV panel by 10% and 18.67%, respectively. Therefore, the use of aluminum heat sinks could provide a potential solution to prevent PV panels from overheating and may indirectly lead to a reduction in CO₂ emissions due to the increased electricity production from the PV system.

1. Introduction

The use of renewable energy resources is of interest to researchers and governments around the world due to increasing energy consumption and climate change issues caused by the exploitation of conventional energy sources [1]. Solar energy is the most abundant renewable energy resource on Earth and could therefore be the solution for the growing demand of global energy consumption [1–3]. In general, the utilization of solar energy is divided into two methods: photothermal and photovoltaic (PV). Photothermal systems utilize the heat energy from solar radiation for various purposes such as crop drying, solar stoves, and solar water heaters [4]. The PV system converts photons from solar radiation directly into electrical energy using solar cell technology [5]. Solar cell technology is widely applied in both small-scale uses, such as street lighting and providing resi-

dential electricity, and large-scale uses such as in national power plants [5–7].

Although solar energy harvesting using solar cell technology is highly promising, there are challenges to maximizing the efficiency of solar cells [8–10]. PV modules based on silicon material can convert 8–20% of solar radiation into electrical energy [11–13] but the rest of the solar radiation is reflected back to the surrounding environment and converted into heat energy that can increase the temperature of the PV device and consequently reduce the total power output [14–16]. Radziemska [12] adjusted the working temperature of solar cells and showed an inverse linear relationship between the temperature and the power output of solar cells. Cotfas and Cotfas [8] found that increasing the temperature of solar cells would degrade the voltage because the electron excitation of the thermal energy was higher than the electrical energy of the semiconductor material. As a

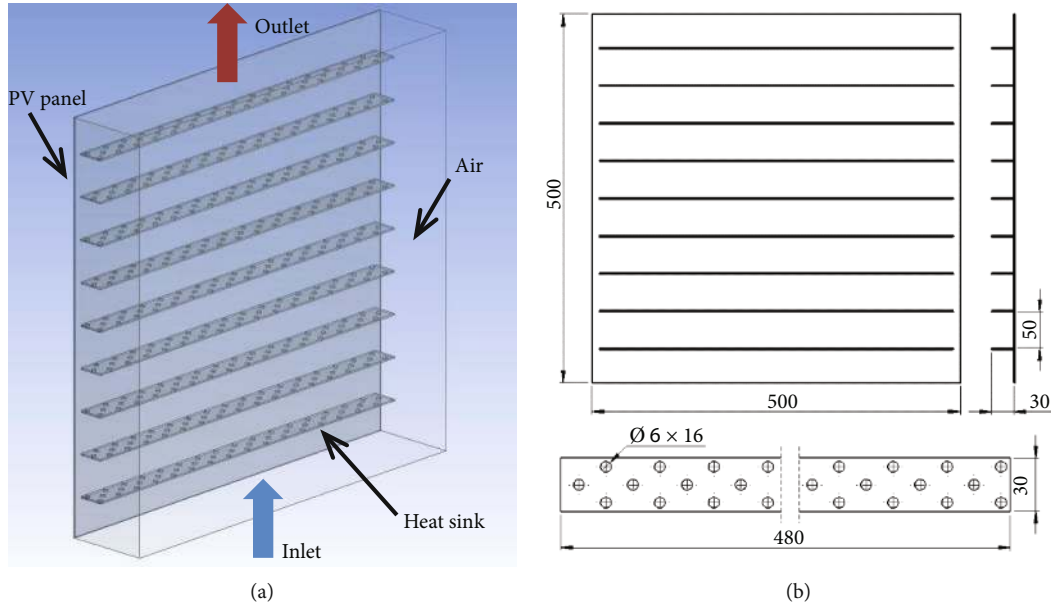


FIGURE 1: The (a) proposed geometry and (b) dimensions of a PV panel with aluminum heat sinks.

result, the efficiency of solar cells with crystalline silicon structures decreases by ± 0.4 – 0.5% for every 1°C increase in temperature [17]. Hence, decreasing the operating temperature of solar cells will be important for achieving a higher efficiency and longer lifespan of these cells [18].

Researchers have developed cooling systems to decrease the operating temperature of solar cells; these are categorized as active and passive cooling systems. Active cooling systems operate mechanical or electrical devices such as fans or pumps, which require external power input, while passive cooling does not require additional power to operate [19–21]. Passive cooling may require additional parts, such as a heat pipe or heat sink, that rely on convective heat transfer to drive coolant flow to the solar cells [22]. A heat sink with thermal conductive material attached to the bottom of a solar cell will increase the area of heat transfer from solar cell to its surrounding environment [17, 22]. Thus, because they are relatively simple and inexpensive to manufacture, heat sinks have a high potential as devices to cool PV panels and should be developed further.

Popovici et al. [23] conducted a simulation using the ANSYS-Fluent software to study the characteristics of heat transfer in a heat sink under turbulent flow conditions. The results showed that the cooling rate of a solar cell was proportional to its fin height and inversely proportional to the configuration of the inclination angle. The temperature of the solar cell was reduced to 10°C and its electrical power capability was increased to 7.55% . Modeling and simulations of heat sinks conducted by Zhu and Sun [24] showed that a simple heat sink can affect the longevity of semiconductor material. Research by Luo et al. [25] used an experimental method to demonstrate several heat sinks with flared fin configurations and obtained an overall reduction in thermal resistance of up to 10% . Research by Grubišić-Čabo et al. [26, 27] examined the aluminum fins mounted on the backside of a PV panel (Si-poly, 50 Wp). The results showed that, under low

wind conditions, the electrical efficiency of solar cells increases by 0.3% and 0.2% under solar irradiation of 850 W/m^2 and 500 W/m^2 , respectively. Based on the various studies currently being conducted on heat sink applications for PV solar cells, there is a great potential to combine simulation and experimental methods to produce an integrated study. This applied research will aid the development of PV cooling systems by providing a complete theoretical and analytical overview of the methods to decrease the temperature of solar cells.

This study investigated the application of heat sinks to a PV module performance with a simple combination of the computational fluid dynamics (CFD) approach and experimental testing. The CFD study was conducted using the ANSYS Fluent software, and the three-dimensional (3D) modeling was carried out to identify the working temperature of the PV module. The results of the simulation were presented as the temperature contour of the module and the velocity profile of the air flowing through the heat sink. The air flow characteristics shown by the velocity profile could provide valuable information regarding the relation between turbulent air flow and the cooling performance of the panel by using an air-cooled heat sink. Additionally, an experimental analysis was performed to study the effects of heat sinks on the electrical characteristics of PV modules. This study also discusses comprehensive physical phenomena in the silicon material of solar cells caused by temperature changes. This heat sink cooling system is expected to decrease operating temperature effectively and increase the efficiency of PV modules.

2. Materials and Methods

2.1. Numerical Setup. Figure 1 shows the design and geometry of a PV module with an aluminum heat sink. The aluminum heat sink was mounted on the back of a vertical solar

TABLE 1: The properties of each layer in the solar module.

Layer	Density (kg/m ³)	Specific heat capacity (kJ/kg K)	Thermal conductivity (W/m K)	Thickness (mm)
Tempered glass	2450	0.79	0.7	3.2
EVA	960	2.09	0.311	0.5
PV cell	2330	0.677	130	0.21
EVA	960	2.09	0.311	0.5
PVF	1200	1.25	0.15	0.3

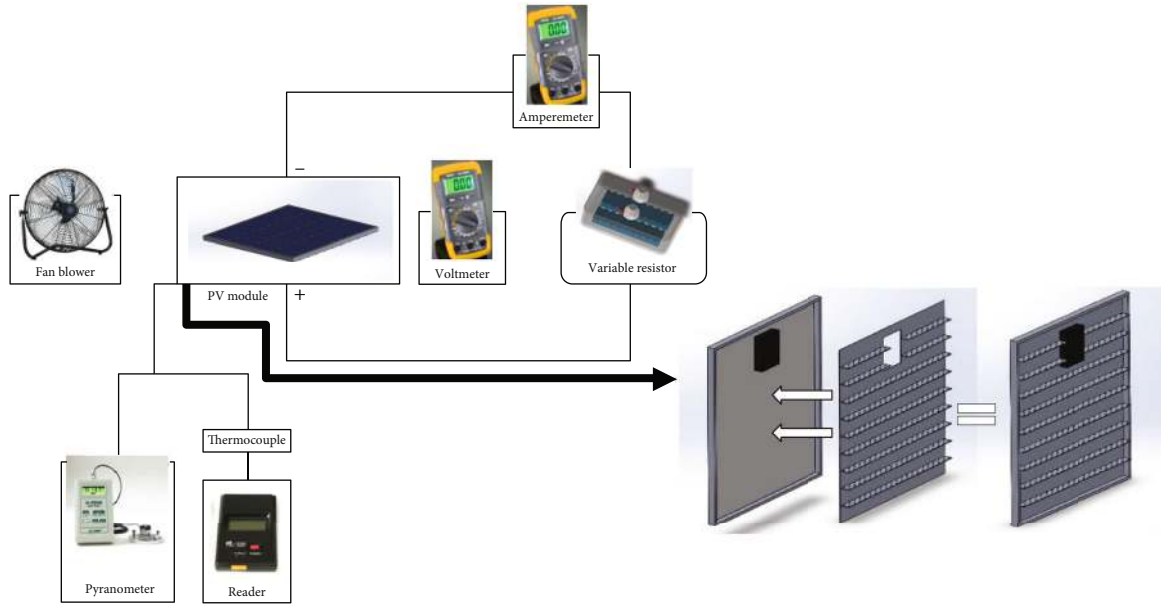


FIGURE 2: Schematic configuration of the PV panel with heat sinks.

panel; the fins of the panel were perforated to improve air circulation around them and allow the absorption of more heat from the PV panel. In the modeling program, the PV panel was assumed to be a unique composite layer [28–30]. Table 1 shows the properties of each layer in the solar module. The properties of these layers are assumed as independent properties with temperature and pressure change.

The base and fins of the heat sink are both 2 mm thick. The fluid domain for air has a width of 0.1 m, with the resulting hydraulic diameter (D) of 0.166 m. The air flow velocity (V) at the inlet was 1.5 m/s, with a temperature of 35°C according to the average temperature and velocity of wind in Indonesia [31–33]. The Reynolds (Re) number and turbulence intensity (I) were calculated using Equations (1) and (2) below:

$$Re = \frac{\rho V D}{\mu} \quad (1)$$

$$I = 0.16 Re^{-1/8} \quad (2)$$

where ρ and μ are density (kg/m³) and viscosity (kg/m s) of fluid, respectively [23]. The Reynolds number for the imposed air velocity was approximately 13100 and the estimated turbulence intensity was 4.8%. The simulation was carried out

under steady-state conditions using the $k-\epsilon$ re-normalization group (RNG) turbulence model. The semi-implicit method for pressure-linked equation (SIMPLE) pressure-velocity coupling and the second-order upwind scheme were used to solve the equations, with convergence criteria of 10^{-6} for energy and 10^{-3} for pressure, velocity, and continuity equations.

The PV panel was irradiated with 1000 W/m² of solar energy in standard test conditions; it converted this into electrical energy through the mechanism of PV effects [34, 35]. In general, the electrical efficiency of the crystalline silicon solar cells ranges from 11 to 20%, while tempered glass reflects as much as 3 to 10% of the solar radiation to the surroundings of the cell. This study assumed that 25% of solar energy is converted into electrical energy and reflected to the environment; therefore, the remaining solar radiation was treated as input heat flux to the solar module [23, 35].

2.2. Experimental Procedure. This study used 50 Wp polycrystalline solar cells with the dimensions of 655 × 670 × 25 mm. The experimental set up is shown in Figure 2, with the aluminum heat sink mounted on the back of a PV panel with fins and a base that are both 2 mm thick. The fins were connected to the baseplate with a rectangular hole to accommodate the PV panel junction box. Before attaching the heat sink to the bottom of the solar panel, the thermal



Note:

- | | |
|--------------------------|------------------------------|
| 1. Fan blower | 5. Solarimeter |
| 2. Anemometer | 6. Voltmeter and amperemeter |
| 3. PV with heat sinks | 7. Variable resistor |
| 4. PV without heat sinks | |

(a)



(b)

FIGURE 3: (a) Photograph of the experimental procedure and (b) heat sink configuration on the back of the PV panel.

grease HT-GY260 (thermal conductivity $> 1.2 \text{ W/m K}$ and thermal impedance $< 0.211 \text{ C-in}^2/\text{W}$) was applied on the contact areas to minimize thermal contact resistance.

The electrical characteristics of the PV panels were measured using a variable resistance method. This method provides an electrical resistance load that varies from zero resistance (to measure the maximum current of a solar cell) to infinite resistance (to measure the maximum voltage of a solar cell). The variable resistance was achieved by arranging several resistors with electrical resistances of 2.5, 3.5, 4.7, 5.4, 5.8, 6.0, 6.4, 6.6, 6.9, 7.4, 8.5, 13.8, 19.6, 42.5, 111, and 330Ω adjusted to the size of the PV panel. A LI-COR LI-250A pyranometer with an accuracy of $\pm 0.6\%$ was used to measure incoming solar irradiation. The temperature of the PV panel was measured with a K-type thermocouple with an accuracy of $\pm 1.2^\circ\text{C}$. The thermocouples were placed on top of the PV panel to measure its average temperature. The wind speed passing through the underside of the PV panel was measured using an anemometer. The position and distance between the 35 W fan blower and the PV panel was adjusted to obtain a uniform wind speed of approximately 1.5 m/s. Figure 3 shows a photograph of the experimental procedure and heat sink configuration on the back of the PV panel.

3. Results and Discussion

3.1. Computational Fluid Dynamics (CFD) Analysis. In the CFD study, the meshing process divided domains into many cells. The cell size varied from big to small such that the meshing process yielded different numbers of elements. This was done to generate independent simulation results not influenced by the number of the cells in the mesh. Meshing was performed with 1 and 2 mm cell size for heat sinks and 4, 6, and 8 mm cell size for the fluid domain. The mesh independence study result had an error of 0.13%.

Figure 4 shows the temperature contour of the PV panel with and without aluminum heat sinks with a heat flux of 1000 W/m^2 . The average temperature for the PV panel without the aluminum heat sinks was 85.3°C and the average temperature for the PV panel with the aluminum heat sinks was 72.8°C . The results showed a significant decrease in temperature down to 12.5°C , and an increase in the heat transfer performance from the panel to the air when aluminum heat sinks are used.

Figure 5 shows the velocity vector of the circulating air which flows through the heat sink. Fins in the heat sink caused turbulence of air flow, so the heat transfer from the

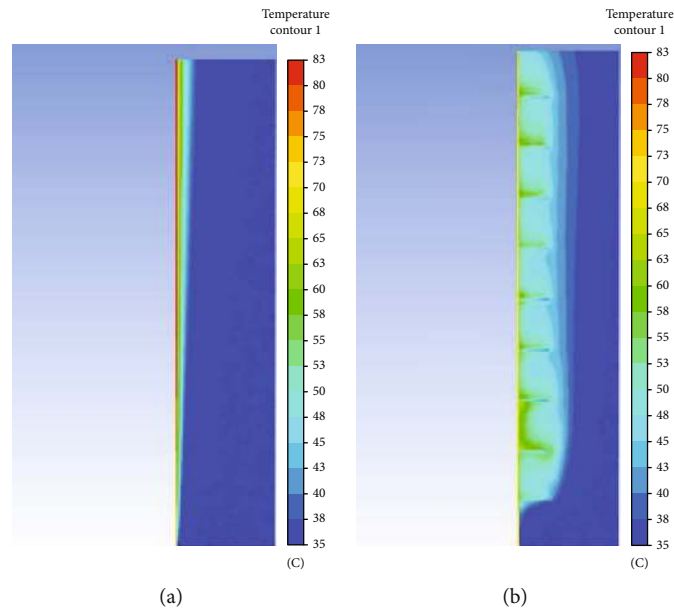


FIGURE 4: Thermal contour of PV panels (a) without aluminum heat sinks and (b) with aluminum heat sinks.

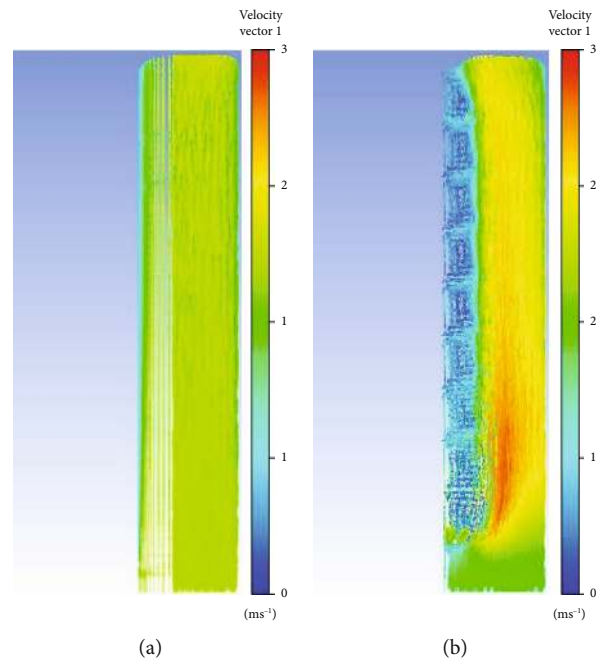


FIGURE 5: Velocity vector of a PV panel (a) without and (b) with aluminum heat sinks.

PV panel to the environment increased. The high turbulence level can reduce the thermal boundary layer thickness and have an impact on the high temperature gradient in the back of the PV panel. As a result, the average temperature of PV panels with heat sinks was lower than in PV panels without heat sinks. Research by Omeroglu [36] revealed a similar result where the heat sink configuration affected the air velocity and heat transfer rate from a PV panel to the surrounding environment. Popovici et al. [23] demonstrated that the orientation and direction of the fin in the heat sink also affected the air temperature distribution. The 0.03 m height of the fin

and 1.5 m/s air inlet velocity decreased the base temperature of the PV panel from 56°C to 42.35°C (ΔT up to 13.65°C), which is similar to this result.

3.2. Experimental Results. Figure 6 shows the average temperature of a PV panel as a function of solar irradiation. As previously noted, the average temperature of a PV panel without a heat sink was higher than that of a PV panel with a heat sink. We also observed that increasing the intensity of solar radiation would consequently increase the temperature of a solar cell. The higher the intensity of the radiation, the

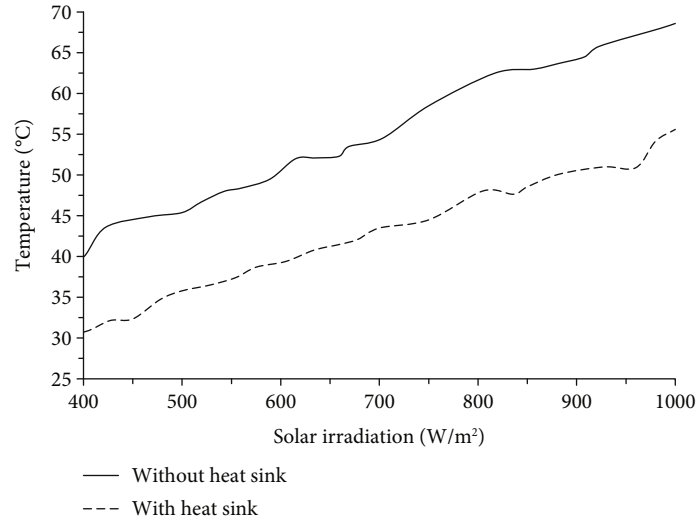


FIGURE 6: Average temperature of a PV panel under various solar irradiation.

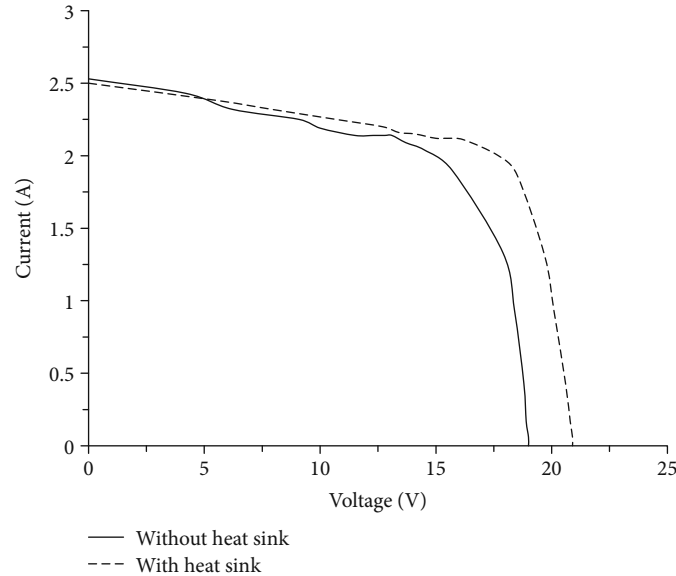


FIGURE 7: I-V curve of PV panel under irradiation of 1000 W/m².

greater the amount of photon energy that hits the solar cell. In turn, a higher amount of photon energy will increase electron excitation in solar panels, which will then result in increasing the temperature of the solar cell [12, 37]. However, the installation of a heat sink increases the heat transfer area and heat transfer rate of a PV panel, thereby reducing the temperature of the panel.

The performance of solar cells can be characterized by a photocurrent-voltage curve (I-V curve) as shown in Figure 7. The measurement results of the I-V curve produce several important parameters, including open-circuit photovoltage (V_{OC}), short-circuit photocurrent (I_{SC}), fill factor (FF), and efficiency (η). This study used a variable resistor system to measure the solar cell characteristics.

V_{OC} is determined at the open-circuit condition or when electrical resistance is very high, with no flow of current

and the voltage at maximum, whereas I_{SC} is determined during the short-circuit condition or when electrical resistance approaches zero and generates a maximum current. The product of current and voltage produces electrical power (P), and the maximum product of current and voltage is called the maximum power point (P_{MPP}). Another important parameter of solar cell performance is the fill factor (FF), which is the ratio of P_{MPP} to the product of V_{OC} and I_{SC} . The efficiency of solar cells (η) is defined as the ratio of P_{MPP} to the solar irradiation energy received by the cells. The electrical characteristics of a PV panel are shown in Table 2.

The heat sink increased the V_{OC} by 10% and reduced the I_{SC} by 1.18%. As the increase in V_{OC} was higher than the decrease in I_{SC} , the electrical power of solar cells also increased. The P_{MPP} from solar cells increased by 18.67%,

TABLE 2: Electrical performance of a PV panel with and without aluminum heat sinks under 1000 W/m² irradiation.

Characteristic	With heat sink	Without heat sink
V_{OC} (volt)	20.9	19
I_{SC} (ampere)	2.5	2.53
P_{MPP} (watt)	35.4	29.83
FF	0.677	0.621
η (%)	11.11	8.51

with the improvement in the electrical performance being primarily caused by the decrease in the operating temperature. The electrical efficiency increase gained with the heat sink could reach 2.6% under 1000 W/m² solar irradiation. Research by Grubišić-Čabo [26, 27] showed a similar trend of increasing efficiency with aluminum fins mounted on the backside of a PV panel (Si-poly, 50 Wp).

Semiconductor properties in solar cells are similar to temperature-sensitive electronic devices. Increasing temperature can decrease the band gap value of the semiconductor, which in turn increases the energy of the electrons in the semiconductor material. As a result, the electron bonds in the semiconductor will be broken easily only by the entry of energy in low quantities. The parameter that is most affected by fluctuations in temperature values is V_{OC} [38, 39]. V_{OC} decreases as operating temperature increases due to the influence of the reverse saturation current (I_0) parameter, as shown in Equations (3), (4), and (5).

$$V_{OC} = \frac{nkT}{q} \ln \left(\frac{I_L}{I_0} \right), \quad (3)$$

$$I_0 = qA \frac{Dn_i^2}{LN_D}, \quad (4)$$

$$I = I_L - I_0 \left(e^{qv/nkT} - 1 \right), \quad (5)$$

where n is the intrinsic carrier concentration (cm⁻³), k is the Boltzman constant (1.381×10^{-23} J/K or 8.617×10^{-5} eV/K), T is the temperature (K), q is the electric charge (1.602×10^{-19} Coulomb), I_L is the current of the solar cell, A is the area of the solar cell, D is the diffusivity of the minority carrier for silicon as a function of doping material, L is the length of diffusivity of the minority carrier, and N_D is the doping material. All of these parameters could change with an increase in temperature, but the most significant change is in the intrinsic carrier concentration as shown in Equations (6) and (7):

$$n_i^2 = BT^3 e^{-E_{GO}/kT}, \quad (6)$$

$$B = 4 \left(\frac{2\pi k}{h^2} \right)^3 (m_e m_h)^{1.5}, \quad (7)$$

where E_{GO} is the band gap energy, h is Planck's constant (6.626×10^{-34} J.s), m_e is the effective mass of the electron, and m_h is the effective mass of the hole. The constant B is

not a function of temperature; therefore, the parameter n depends on the operating temperature of the semiconductor. Semiconductors with low band gap values will produce a high intrinsic carrier concentration; thus, they will also produce high n values at high temperatures. The intrinsic carrier concentration value of silicon material can be determined as a function of temperature as shown in Equation (8) [40]:

$$n_i(T) = 5.29 \times 10^{19} \left(\frac{T}{300} \right)^{2.54} e^{-6726/T} \quad (8)$$

Based on Equations (3) and (4), a high n value produces a large reverse saturation current (I_0) value, thereby reducing the V_{OC} value of the solar cell. Additionally, Equation (5) indicates that the increase in the values of I_0 and n will result in an increase in the current. However, the increase in the current is negligible compared to the decrease in voltage from the solar cell [41].

In addition to the changing current and voltage values, changes in the operating temperature of the solar cell also affect the fill factor (FF). The rise in temperature increases the internal resistance of solar cells, and these obstacles contribute to the charge flow at the p - n junction, resulting in a loss in the form of charge recombination in the cell. This decreases FF when the operating temperature of solar cells increases. Therefore, because the output power of a solar cell is the product of voltage and current, an increase in temperature will result in a decrease in power [11, 12].

4. Conclusions

We conducted a CFD simulation for PV panels with and without aluminum heat sinks installed. The results showed a reduction of up to 10°C in the average temperature of the PV panels with a heat sink. A physical experiment was also conducted with a PV module that had a heat sink installed, and various values of solar irradiation were applied to PV module to observe their influence on the temperature distribution of the PV panel. The results showed that the installed heat sink could reduce the panel temperature due to the increased heat transfer area and heat transfer performance. Because of its decreasing temperature, the heat sink increased the V_{OC} and P_{MPP} of the PV panel by 10% and 18.67%, respectively. The simple design of this heat sink model provides a potential solution to prevent PV panels from overheating and may indirectly lead to a reduction in CO₂ emissions due to the increased electricity production from the PV system. However, the analysis could be developed further from the economic perspective, to produce a cost-based and performance-based optimum design for heat sinks.

Data Availability

The data used to support the findings of this study are available from the corresponding author upon request.

Conflicts of Interest

The authors state that there are no conflicts of interest to declare.

Acknowledgments

This research was funded by the Direktorat Penelitian dan Pengabdian kepada Masyarakat (DP2M), Direktorat Jenderal Pendidikan Tinggi (DIKTI) (research grant number 719/UN27.21/PN/2019). The authors are grateful to Ian Guardian for his assistance during the research.

References

- [1] N. Kannan and D. Vakeesan, "Solar energy for future world: -a review," *Renewable and Sustainable Energy Reviews*, vol. 62, pp. 1092–1105, 2016.
- [2] K. Gairaa and Y. Bakelli, "Solar energy potential assessment in the Algerian South Area: Case of Ghardaia Region," *Journal of Renewable Energy*, vol. 2013, Article ID 496348, 11 pages, 2013.
- [3] K. Jager, O. Isabella, A. H. M. Smets, R. A. C. M. M. Swaaijvan, and M. Zeman, *Solar Energy: Fundamentals, Technology and Systems*, Delft University of Technology, 2014.
- [4] X. Wu, G. Y. Chen, G. Owens, D. Chu, and H. Xu, "Photothermal materials: a key platform enabling highly efficient water evaporation driven by solar energy," *Materials Today Energy*, vol. 12, pp. 277–296, 2019.
- [5] L. Fraas and L. Partain, "Summary, conclusions, and recommendations," in *Solar Cells and their Applications, Second Edition*, pp. 581–611, John Wiley & Sons, Inc, 2010.
- [6] T. Hanada, "Modifying the feed-in tariff system in Japan : an environmental perspective," *Evergreen*, vol. 3, no. 2, pp. 54–58, 2016.
- [7] Z. Arifin, S. Soeparman, D. Widhiyanuriyawan, and S. Suyitno, "Performance enhancement of dye-sensitized solar cells using a natural sensitizer," *International Journal of Photoenergy*, vol. 2017, Article ID 2704864, 5 pages, 2017.
- [8] D. T. Cotfas and P. A. Cotfas, "Multiconcept methods to enhance photovoltaic system efficiency," *International Journal of Photoenergy*, vol. 2019, Article ID 1905041, 14 pages, 2019.
- [9] A. Alkhalidi, M. K. Khawaja, and A. G. al Kelany, "Investigation of repurposed material utilization for environmental protection and reduction of overheating power losses in PV panels," *International Journal of Photoenergy*, vol. 2019, Article ID 2181967, 9 pages, 2019.
- [10] A. Gaur and G. N. Tiwari, "Performance of photovoltaic modules of different solar cells," *Journal of Solar Energy*, vol. 2013, Article ID 734581, 13 pages, 2013.
- [11] S. Dubey, J. N. Sarvaiya, and B. Seshadri, "Temperature dependent photovoltaic (PV) efficiency and its effect on PV production in the world-a review," *Energy Procedia*, vol. 33, pp. 311–321, 2013.
- [12] E. Radziemiska, "The effect of temperature on the power drop in crystalline silicon solar cells," *Renewable Energy*, vol. 28, no. 1, pp. 1–12, 2003.
- [13] D. T. Cotfas, P. A. Cotfas, and O. M. Machidon, "Study of temperature coefficients for parameters of photovoltaic cells," *International Journal of Photoenergy*, vol. 2018, Article ID 5945602, 12 pages, 2018.
- [14] M. Ozgoren, M. H. Aksoy, C. Bakir, and S. Dogan, "Experimental performance investigation of photovoltaic/thermal (PV-T) system," *EPJ Web of Conferences*, vol. 45, article 01106, 2013.
- [15] K. Chumpolrat, V. Sangsuwan, N. Udomdachanut et al., "Effect of ambient temperature on performance of grid-connected inverter installed in Thailand," *International Journal of Photoenergy*, vol. 2014, Article ID 502628, 6 pages, 2014.
- [16] T. T. Thao, T. Q. Trung, V. V. Truong, and N. N. Dinh, "Enhancement of power efficiency and stability of P3HT-based organic solar cells under elevated operating-temperatures by using a nanocomposite photoactive layer," *Journal of Nanomaterials*, vol. 2015, Article ID 463565, 7 pages, 2015.
- [17] S. Wu and C. Xiong, "Passive cooling technology for photovoltaic panels for domestic houses," *International Journal of Low-Carbon Technologies*, vol. 9, no. 2, pp. 118–126, 2015.
- [18] H. Chen, X. Chen, S. Chu, L. Zhang, and Y. Xiong, "Numerical and experimental study on energy performance of photovoltaic-heat pipe solar collector in northern China," *International Journal of Photoenergy*, vol. 2015, Article ID 321829, 8 pages, 2015.
- [19] H. A. Hussien, M. Hasanuzzaman, A. R. Abdulmunem, and A. H. Noman, "Enhance photovoltaic/thermal system performance by using nanofluid," in *3rd IET International Conference on Clean Energy and Technology (CEAT) 2014*, pp. 5–9, Kuching, Malaysia, 2014.
- [20] M. Hasanuzzaman, A. B. M. A. Malek, M. M. Islam, A. K. Pandey, and N. A. Rahim, "Global advancement of cooling technologies for PV systems: a review," *Solar Energy*, vol. 137, pp. 25–45, 2016.
- [21] R. Mazón-Hernández, J. R. García-Cascales, F. Vera-García, A. S. Káiser, and B. Zamora, "Improving the electrical parameters of a photovoltaic panel by means of an induced or forced air stream," *International Journal of Photoenergy*, vol. 2013, Article ID 830968, 10 pages, 2013.
- [22] D. Sato and N. Yamada, "Review of photovoltaic module cooling methods and performance evaluation of the radiative cooling method," *Renewable and Sustainable Energy Reviews*, vol. 104, pp. 151–166, 2019.
- [23] C. G. Popovici, S. V. Hudîşteanu, T. D. Mateescu, and N. C. Cherecheş, "Efficiency improvement of photovoltaic panels by using air cooled heat sinks," *Energy Procedia*, vol. 85, pp. 425–432, 2016.
- [24] J. Zhu and L. Sun, "Modelling and numerical simulations of heat distribution for LED heat sink," *Discrete Dynamics in Nature and Society*, vol. 2016, Article ID 3468246, 8 pages, 2016.
- [25] Q. Luo, P. Li, L. Cai et al., "Experimental investigation on the heat dissipation performance of flared-fin heat sinks for concentration photovoltaic modules," *Applied Thermal Engineering*, vol. 157, article 113666, 2019.
- [26] F. Grubišić-Čabo, S. Nižetić, D. Čoko, I. Marinić Kragić, and A. Papadopoulos, "Experimental investigation of the passive cooled free-standing photovoltaic panel with fixed aluminum fins on the backside surface," *Journal of Cleaner Production*, vol. 176, pp. 119–129, 2018.
- [27] F. Grubišić-Čabo, S. Nižetić, I. Marinić Kragić, and D. Čoko, "Further progress in the research of fin-based passive cooling technique for the free-standing silicon photovoltaic panels," *International Journal of Energy Research*, vol. 43, no. 8, pp. 3475–3495, 2019.

- [28] L. Liu, Q. Wang, H. Lin, H. Li, Q. Sun, and R. Wennersten, "Power generation efficiency and prospects of floating photovoltaic systems," *Energy Procedia*, vol. 105, pp. 1136–1142, 2017.
- [29] S. Armstrong and W. G. Hurley, "A thermal model for photovoltaic panels under varying atmospheric conditions," *Applied Thermal Engineering*, vol. 30, no. 11–12, pp. 1488–1495, 2010.
- [30] B. Sutanto and Y. S. Indartono, "Numerical approach of Al_2O_3 -water nanofluid in photovoltaic cooling system using mixture multiphase model," *IOP Conference Series: Earth and Environmental Science*, vol. 168, article 012003, 2018.
- [31] S. Hudisteanu, T. Mateescu, C. Popovici, and N.-C. Chereces, "Numerical study of air cooling photovoltaic panels using heat sinks," *Romanian Journal of Civil Engineering*, vol. 6, pp. 11–21, 2015.
- [32] E. Data, *Global Wind Atlas Mean Wind Speed Map*, , energy-data.info, 3, 2019, <https://globalwindatlas.info/>.
- [33] M. Ali, M. H. Iqbal, N. A. Sheikh et al., "Performance investigation of air velocity effects on PV modules under controlled conditions," *International Journal of Photoenergy*, vol. 2017, Article ID 3829671, 10 pages, 2017.
- [34] M. A. Bashir, H. M. Ali, S. Khalil, M. Ali, and A. M. Siddiqui, "Comparison of performance measurements of photovoltaic modules during winter months in Taxila, Pakistan," *International Journal of Photoenergy*, vol. 2014, Article ID 898414, 8 pages, 2014.
- [35] B. Sutanto and Y. S. Indartono, "Computational fluid dynamic (CFD) modelling of floating photovoltaic cooling system with loop thermosiphon," in *AIP Conference Proceedings*, vol. 020011, Bali, Indonesia, 2019.
- [36] G. Ömeroğlu, "CFD analysis and electrical efficiency improvement of a hybrid PV/T panel cooled by forced air circulation," *International Journal of Photoenergy*, vol. 2018, Article ID 9139683, 11 pages, 2018.
- [37] M. S. Hossain, R. Saidur, H. Fayaz et al., "Review on solar water heater collector and thermal energy performance of circulating pipe," *Renewable and Sustainable Energy Reviews*, vol. 15, no. 8, pp. 3801–3812, 2011.
- [38] C. Honsberg and S. Bowden, "PV Education.org 2018," <https://www.pveducation.org>.
- [39] D. M. Tobnaghi and D. Naderi, "The effect of solar radiation and temperature on solar cells performance," *Extensive Journal of Applied Sciences*, vol. 3, no. 2, pp. 39–43, 2015.
- [40] K. Misiakos and D. Tsamakis, "Accurate measurements of the silicon intrinsic carrier density from 78 to 340 K," *Journal of Applied Physics*, vol. 74, no. 5, pp. 3293–3297, 1993.
- [41] D. M. Tobnaghi, R. Madatov, and P. Farhadi, "Investigation of light intensity and temperature dependency of solar cells electric parameters," in *Electric Power Engineering & Control Systems 2013*, pp. 21–23, Lviv, Ukrain, November 2013.

